Excitonic properties in (111)B-grown (In,Ga)As/GaAs piezoelectric multiple quantum wells

P. Ballet,* P. Disseix, J. Leymarie, A. Vasson, and A-M. Vasson
Laboratoire des Sciences et Matériaux pour l'Electronique, et d'Automatique, Unité Mixte de Recherche No. 6602 du Centre National de la Recherche Scientifique, Université Blaise Pascal Clermont-Ferrand II, 63177 Aubière Cedex, France

R. Grey
Department of Electronic and Electrical Engineering, University of Sheffield, Sheffield S1 4DU, United Kingdom
(Received 21 July 1997)

The excitonic properties in two (111)B-grown $In_{0.15}Ga_{0.85}As$ multiple quantum well p-i-n diodes, with 7 and 14 quantum wells, respectively, are investigated by thermally detected optical absorption (TDOA) and by electroreflectance (ER) as a function of applied bias, the latter modifying the electric-field distribution in the heterostructure. The line shapes of the ER signals are analyzed by means of a multilayer model enabling the energies and the oscillator strengths of excitons to be deduced while the direct measurements of the energy positions of the TDOA peaks provide an accurate determination of the excitonic transition energies at zero-voltage applied bias. The excitonic characteristics are calculated by using a variational approach with a two-parameter trial function. The piezoelectric field in the strained $In_xGa_{1-x}As$ layers is determined by including the excitonic contribution. The theoretical oscillator strengths are compared to those obtained from ER experiments for several excitonic transitions; all the physical trends are well reproduced but it appears that a quantitative agreement cannot be found without taking into account the in-plane valence-band mixing. A study is also presented for the optimization of optoelectronic devices by means of a figure of merit that combines the oscillator strength of the fundamental excitonic transition and the ability for such devices to produce the largest energy shift for a 1-V additional applied bias. [S0163-1829(97)04447-0]

I. INTRODUCTION

The growth of semiconducting strained layers on high index planes has enabled a further field of investigation to be explored in the physics of heterostructures due to the presence of a strong internal piezoelectric field. This piezoelectric field results from the displacement of the anion and cation sublattices induced by the off-diagonal terms in the deformation tensor and is consequently absent in the case of growth on conventional (100) substrates. The (111) orientation offers the possibility to produce the largest piezoelectric field, which can easily exceed 100 kV cm^{-1};[1] in addition, the critical thickness is increased with respect to the (100) growth and thus enables thicker multiple quantum-well structures to be grown.[2]

The effects of such a strong piezoelectric field on the band structure, leading to large energy shifts and to optical nonlinearity, are used to design electro-optic devices.[3–5] The optimization of their performances imposes the knowledge of the piezoelectric field effects on the excitonic properties in such structures. The most important consequence of the in-well electric field is the reduction of the electron and hole wave-function overlap by pushing back the carriers to the opposite sides of the well. This phenomenon induces large decreases in the exciton binding energy and oscillator strength of the fundamental exciton. It is enhanced when the well is thick and can even lead to the formation of a quasi-type-II configuration.[6]

Another important effect of the internal electric field is breaking of the symmetry along the growth direction. In this case, transitions forbidden from the classical selection rules are now allowed and the associated oscillator strengths can be larger than that of the fundamental exciton if the in-well field is sufficiently strong (typically 100 kV cm^{-1}).

Since the electro-optic devices mentioned above use the quantum-confined Stark effect (QCSE), which produces a large energy shift of the band edge, their efficiency could be proportional to the magnitude of the in-well electric field. However, the larger the piezoelectric field the larger the fall in the oscillator strength for the fundamental excitonic transition that dominates the band edge.

In this work, in order to detect the different excitonic transitions, we have carried out thermally detected optical absorption (TDOA) and electroreflectance (ER) experiments on two $In_xGa_{1-x}As/GaAs$ multiple-quantum-well p-i-n diodes grown on (111)B substrates. The piezoelectric field is determined by compensating the in-well field by means of a bias voltage. The effects of the piezoelectric field on the excitonic properties are investigated through a variational method. The oscillator strengths for the fundamental and some excited transitions, determined from our experiments and calculated theoretically, are compared within the range of the reverse applied bias investigated. Finally, in order to determine quantitatively the capability of piezoelectric heterostructures to produce the largest energy shifts combined with the largest oscillator strength, we present a figure of merit. This characterizes the type of structure investigated here; it is equivalent to that defined by Rodriguez-Girones and Rees for all optical non-linear devices.[7]

II. EXPERIMENTAL DETAILS

$In_{0.15}Ga_{0.85}As/GaAs$ multiple quantum well p-i-n diodes have been grown by molecular beam epitaxy on the B face of

n^+ (111) GaAs substrates tilted by 2° towards $(2\bar{1}\bar{1})$ for an enhanced crystal quality.[8] The n^+ and surface p^+ layers of the diodes consist of 3-μm GaAs, Si and Be doped, respectively; the nominal dopant concentrations, confirmed by $C(V)$ measurements are 2×10^{18} cm^{-3}. Wells of 100 Å width are incorporated centrally in the intrinsic GaAs region and are separated by 150-Å GaAs barriers. Details concerning growth conditions are available in Ref. 9.

The two samples investigated here differ only by the number of wells N, namely, 7 in sample 1 and 14 in sample 2. The length (7350 Å) of the intrinsic region is the same for the two samples leading to an equivalent built-in electric field. In order to allow for the potential drop across the diodes, the electric fields are shared between the wells and barriers as described by Pabla *et al.*[10] This sharing of the piezoelectric field induces a larger in-well field in the sample containing the smallest number of wells leading to a stronger QCSE. In this way, the excitonic transition energies in sample 1 are expected to be smaller than those in sample 2.

TDOA is a nonconventional technique based on the detection of the temperature rise of the sample caused by phonon emission due to nonradiative de-excitation occurring after optical absorption. This heating is detected at liquid-helium temperatures (typically 0.35 K) by a germanium resistor thermometer. This method enables temperature variations much less than 10^{-3} K to be detected and it is thus very appropriate for studying weak absorptions occurring in the high electric field regime. The monochromatic light source is a halogen lamp followed by a HR 640 Jobin-Yvon monochromator, which provides a weak excitation power that prevents any optical screening of the in-well electric field. Details concerning the experimental setup are available in Refs. 11 and 12.

ER experiments are performed at 4 K on sample pieces in the form of 400-μm-diameter annular diodes with a 200-μm optical access. The modulation source is a square alternative voltage of amplitude 0.5 V. In order to balance the in-well field, we superimpose a bias dc voltage. The excitation source is a halogen lamp; the optical screening is limited by the addition of a filter that stops photons of energy larger than that of the barrier gap. The modulated signal is analyzed through the HR640 monochromator and detected with a liquid-nitrogen-cooled germanium detector using a standard lock-in amplification.

III. EXPERIMENTAL RESULTS

The TDOA spectra of the two samples are displayed in Fig. 1. In order to make the analysis easier we have simulated the monotonic increase, with photon energy, of the TDOA signal by a polynomial curve and subsequently eliminated it by a simple subtraction. This increase of the TDOA signal is attributed to the impurity absorption front of the GaAs barriers.

For the two samples investigated, four transitions, involving the first (e_1) and second (e_2) levels of electrons and the first (hh_1), second (hh_2), and third (hh_3) levels of heavy holes are detected. For sample 2, the wide structure observed at higher energy corresponds to the superposition of several transitions such as e_2hh_2, e_1hh_4,..., which are close in energies and in oscillator strengths. It is worth noting that the

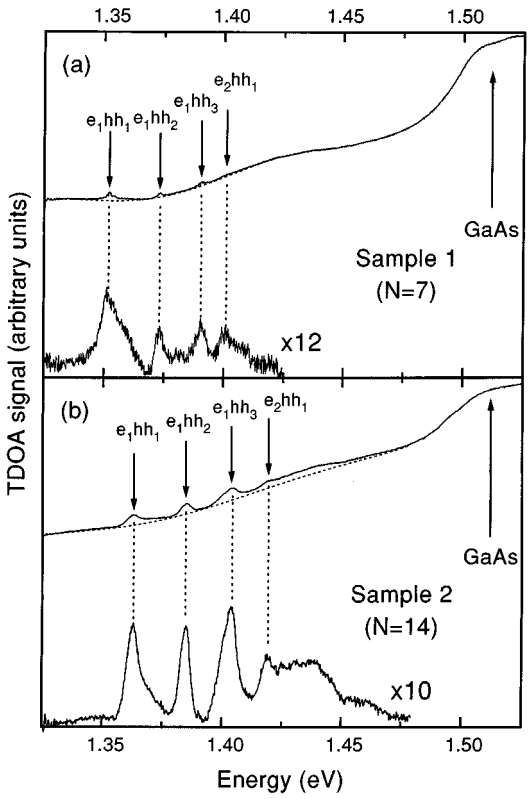

FIG. 1. TDOA spectra of sample 1 ($N=7$) (a) and sample 2 ($N=14$) (b). To facilitate the analysis, a baseline (dashed) corresponding to the impurity absorption front of the GaAs barriers has been removed. The result of the subtraction is shown after amplification at the bottom of each part of the figure.

intensities of the transitions forbidden from the classical selection rules may be of the same order of magnitude as those of the allowed transitions; this is the signature of the presence of a large in-well electric field.

As expected, the transition energies of sample 1, containing only 7 wells, are redshifted by a few meV with respect to those of sample 2. This fact confirms that the electric field is larger in the wells of sample 1 and offers the possibility to tailor this in-well field by a simple modification of the number of wells in such heterostructures.

Figure 2 shows the evolution of the ER spectra of sample 1 when the applied bias is varied from 0 to 12 V. The inset indicates how this bias influences the band structure; the applied electric field balances progressively the in-well field until reaching the flat well conditions and then reverses it. The spectra are noisy because of the reduced optical access imposed by the processing of the samples but excitonic features associated with GaAs and with confined states up to e_2hh_2 are well defined. One can follow the position and intensity changes of the fundamental exciton signal from 1.5 to 12 V; the maximum in the transition energy indicates that the flat band configuration in the wells has been reached. This situation occurs for voltages near to 10 V. In this case, the lack of in-well electric field leads to the vanishing of the forbidden transitions. At lower voltages, the fundamental and excited transitions can be detected together. For a 3-V applied bias, their intensities are of the same order; for a smaller applied bias, corresponding to larger in-well field,

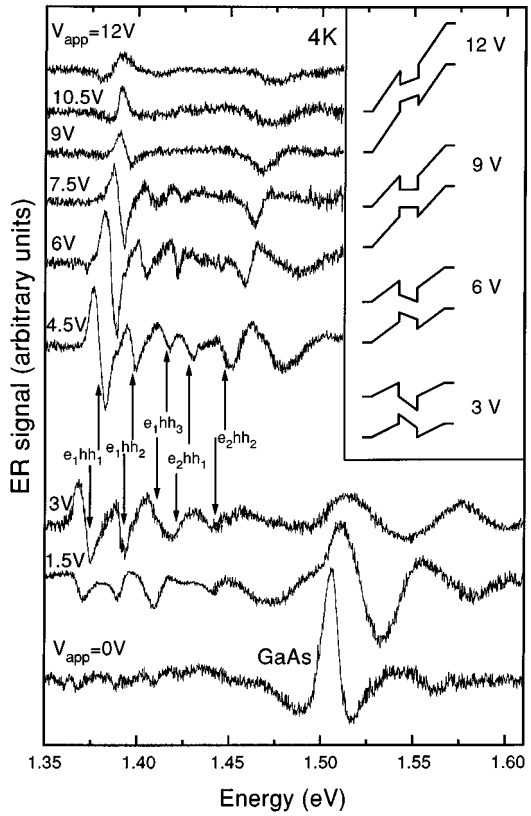

FIG. 2. ER spectra of sample 1 for different values of applied bias (V_{app}) between 0 and 12 V. Spectra are shifted for clarity. The inset shows the potential profiles of one of the wells for different values of applied voltage.

the magnitudes of the forbidden transitions become stronger than that of the fundamental transition. However, for the largest in-well fields (without applied bias), all transitions associated with the wells disappear. This shows that for very strong electric fields, all transition probabilities are weak. This vanishing of the excitonic features of the wells can be also related to the strong GaAs excitonic signal, which indicates that many carriers recombine in the barrier region where the electric field is weaker.

Another effect of increasing the bias is the increase of the barrier field. From the top part of the inset in Fig. 2 it can be seen that, for a strong barrier electric field, the potential discontinuity forms a tip through which the carriers may escape. In this case, the states are no longer quasibound but become resonant. This phenomenon is responsible for the damping of the excitonic features and leads to their complete vanishing for applied voltages larger than 12 V.

In order to have a precise knowledge of the energy positions of all excitonic transitions in the ER spectra, we have used a model that is based on a calculation of the reflection coefficient r and on the determination of its variations with electrical modulation. The reflection coefficient is written algebraically by considering the different reflections and transmissions at the interfaces between successive layers of different optical indices taking into account the different dephasing terms provided when the light goes through the layers of the heterostructure. The reflectance R can be expressed as the square modulus of the reflection coefficient and taken as a function of the real and imaginary parts of the dielectric function ϵ_1 and ϵ_2 in the form

$$R(\epsilon_1,\epsilon_2)=rr^*.$$

The modulation voltage in the ER experiments modifies the electric field inside the sample and thus also modifies the reflectance by mean of the dielectric function. In the case of heterostructures, the change in reflection can be expressed in terms of the first derivative of the dielectric function leading to the well-known expression[13]

$$\frac{\Delta R}{R}=\frac{1}{R}\frac{\partial R}{\partial \epsilon_1}\Delta\epsilon_1+\frac{1}{R}\frac{\partial R}{\partial \epsilon_2}\Delta\epsilon_2.$$

It can be written algebraically by one derivative of the reflectance with respect to ϵ_1 and ϵ_2. Finally, the dielectric function is modeled by a standard damped Lorentzian oscillator including three adjustable parameters: $E_{\rm exc}$, which is the energy of the oscillator, γ, a phenomenological damping parameter, and A, the integrated intensity. The latter can be related to the oscillator strength by matching the absorption coefficient obtained from classical and semiclassical theories.[14]

A change in the electric field ΔF induced by a change in the modulated voltage ΔV leads to a modification in the dielectric function given by

$$\Delta\epsilon=\frac{\partial\epsilon}{\partial E_{\rm exc}}\left[\frac{\partial E_{\rm exc}}{\partial F}\right]\Delta F+\frac{\partial\epsilon}{\partial\gamma}\left[\frac{\partial\gamma}{\partial F}\right]\Delta F+\frac{\partial\epsilon}{\partial A}\left[\frac{\partial A}{\partial F}\right]\Delta F.$$

The three terms in square brackets correspond to the different mechanisms of modulation and give the shape of the spectra.

Modulation spectroscopy is a relevant technique for our study because the magnitudes of the excitonic signals obtained depend upon the modulation efficiencies.[15] Since the modulation spectra in the case of heterostructures are of first derivative type and since the dominating modulation mechanism involves the excitonic energy $E_{\rm exc}$,[13] the magnitude can be expressed as the product $f_{\rm osc}(\partial E_{\rm exc}/\partial F)$ where $f_{\rm osc}$ is the oscillator strength of the excitonic transition. In this way, it is expected that no transitions could be detected for the bias corresponding to the exact flat well because the term $\partial E_{\rm exc}/\partial F$ vanishes. This can be used to locate the flat band configuration with a high precision leading to an accurate determination of the in-well field strength. Unfortunately, we have never found such a flat spectrum. This is due to the fact that the band structure is not perfectly symmetric because of the presence of a strong barrier electric field. In addition, for such a bias, the damping of the excitonic features increases, leading to the contribution of the second modulation term $\partial\gamma/\partial F$.

IV. THEORY

We have considered a free-standing heterostructure so that the strain is entirely accommodated by the quantum wells.[16] The strain tensor has been determined from the formalism described by Yang *et al.* giving analytical expressions of the deformation tensor for an arbitrarily oriented substrate.[17] We have applied this formalism to the case of a

TABLE I. Parameters used to calculate the transition energies.

	a_0 (Å)	C_{11} (N/m^2)	C_{12} (N/m^2)	C_{44} (N/m^2)	a (eV)	d (eV)	me (m_0)	γ_1	γ_3	Δ_{so} (eV)	ϵ
InAs	6.0584[a]	8.33[a]	4.53[a]	3.96[a]	−5.9[a]	−3.6[a]	0.060c	19.67[a]	2.73[a]	0.380[a]	15.15[a]
GaAs	5.6533a	11.88[a]	5.38[a]	5.99[a]	−8.16[b]	−5.4[a]	0.0667[a]	6.85[a]	9.29[a]	0.341[a]	12.50[a]

[a]Reference 18.
[b]Reference 19.
[c]Reference 20.

pure [111] direction and to that of a tilt of 2° towards the [21 1] direction and found a piezoelectric field difference less than 1% between the two cases. Therefore, we have only considered the case of a pure (111)B growth axis to investigate theoretically the electronic properties of such systems.

The parameters used for the calculation of the transition energies are listed in Table I. The effective masses of the heavy holes in the growth direction are determined from the Luttinger-Kohn Hamiltonian $[m_{hh\perp}=m_0/(\gamma_1-2\gamma_3)]$.[21] The light holes play no role in our spectroscopy results because they are resonant with the GaAs barriers for the indium composition investigated. The effective masses for electrons are those related to the (100) growth axis assuming that the effect of the growth direction on the band structure is mainly confined to the valence band.[22,23] The effects of the strain on the energy gap are taken into account;[24] the unstrained well gap is deduced from the Goetz relation.[25] All the alloy parameters are deduced from those of the binary constituents by using Vegard's law.

To calculate eigenenergies and the associated wave functions, we have used a staircase approximation within the transfer matrix formalism, which is very appropriate to study irregular potentials such those provided by electric fields.[26] The potential is discretized in stairs; the length of one stair is typically the monolayer thickness and its height represents the potential variation induced by the electric field.

In order to evaluate the effects of strong internal electric fields on the excitonic properties, the transfer matrix formalism has been combined with a variational method.[27,28] The total Hamiltonian of the exciton H_{exc} can be expressed as a sum of three contributions:

$$H_{exc}=H_e+H_h+H_{eh}.$$

H_e and H_h are the classical Hamiltonians of the electron and the hole in the presence of a longitudinal electric field and H_{eh} contains the kinetic energy and Coulomb terms such that

$$H_{eh}=-\frac{\hbar^2}{2\mu}\Delta\rho-\frac{e^2}{4\pi\epsilon\epsilon_0 r},$$

where r is the distance between the two carriers, ρ is the radial component in the cylindrical coordinates, μ represents the reduced exciton effective mass in the layer plane and ϵ is the relative dielectric constant.

The hole in-plane effective mass is determined by neglecting the longitudinal component of the wave-vector in the Luttinger Hamiltonian. This approximation leads to the expression $m_{hh\parallel}=m_0/(\gamma_1+\gamma_3)$; the implications of this approximation are discussed in the next section. The dielectric constant in the $In_xGa_{1-x}As$ layers is determined by a linear interpolation (see Table I).

The excitonic trial wave function contains two variational parameters α and λ and takes the form:

$$\Phi_{exc}(z_e,z_h,\rho)=\varphi_e(z_e)\varphi_h(z_h)\exp\left(-\frac{\sqrt{\rho^2+\alpha(z_e-z_h)^2}}{\lambda}\right).$$

z_e, z_h, φ_e, and φ_h are the coordinates of the electron and hole along the quantization direction and their envelope functions, respectively. The parameter λ is a measure of the exciton Bohr radius and α stands for the exciton dimensionality. The limiting two-dimensional (2D, $\alpha=0$) and three-dimensional (3D, $\alpha=1$) excitons in an $In_xGa_{1-x}As/GaAs$ quantum well, in the presence of longitudinal internal electric fields, have been studied frequently,[29,30] but André *et al.* have shown that α takes intermediate values in the case of II-VI compounds.[6]

The binding energy is calculated numerically by minimizing the total energy of the exciton. The oscillator strength is then deduced from the expression:

$$f_{osc}\propto\frac{\langle\varphi_e(z_e)|\varphi_h(z_h)\rangle^2}{\langle\Phi_{exc}|\Phi_{exc}\rangle}.$$

The variations with the well width have been calculated for an $In_{0.15}Ga_{0.85}As$ quantum well, with 120 kV cm^{-1} in-well field (F_w) and 40 kV cm^{-1} barrier opposite field (F_b) and are plotted in Fig. 3 for the fundamental and first excited excitons. The lowest limit for thicknesses is 30 Å because the electrons become no longer localized in the well but escape through the potential tips induced by the barrier field. The results are compared to these for a fundamental exciton in an equivalent structure without any electric field. One can see that the binding energy and oscillator strength of excitons strongly decrease with well width because of the enhanced carrier separation leading to a quasi-type-II configuration. For thicknesses larger than 150 Å, the e_1hh_1 and e_1hh_2 wave-function overlap reaches a zero value. With increasing well width, the dimensionality parameter α first follows the evolution of that in a square quantum well in the region where the confinement effects are predominant; the electric-field perturbation is not seen by the carriers that are strongly delocalized for small well widths. Note that, in this case, the major effect of an electric field in a quantum structure, which is to allow transitions forbidden from classical selection rules, vanishes. When the thickness increases above 100 Å, the electrons and holes are pushed towards opposite sides of the quantum well leading to a drastic decrease of the Cou-

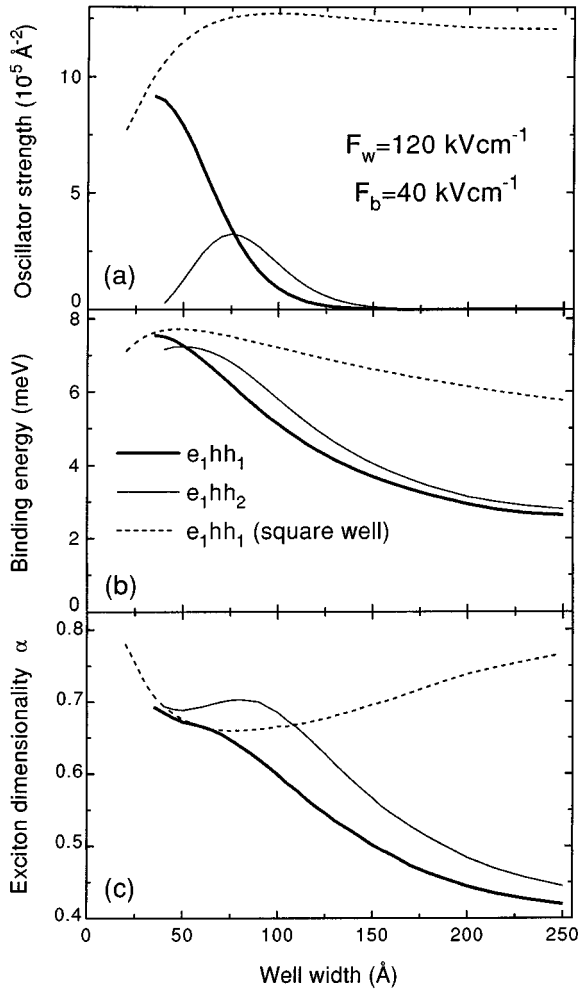

FIG. 3. Variations with well width of the oscillator strength (a), binding energy (b), and exciton dimensionality (c) obtained with the two variational parameter excitonic trial function. Solid lines correspond to e_1hh_1 (thick lines) and e_1hh_2 (thin lines) excitons in a piezoelectric quantum well in the intrinsic region of a *p-i-n* diode and the dashed lines represent the results calculated for a perfect square well with equivalent characteristics. The electric field limits the study to well width larger than 30 Å; under this limit the states are no longer bound.

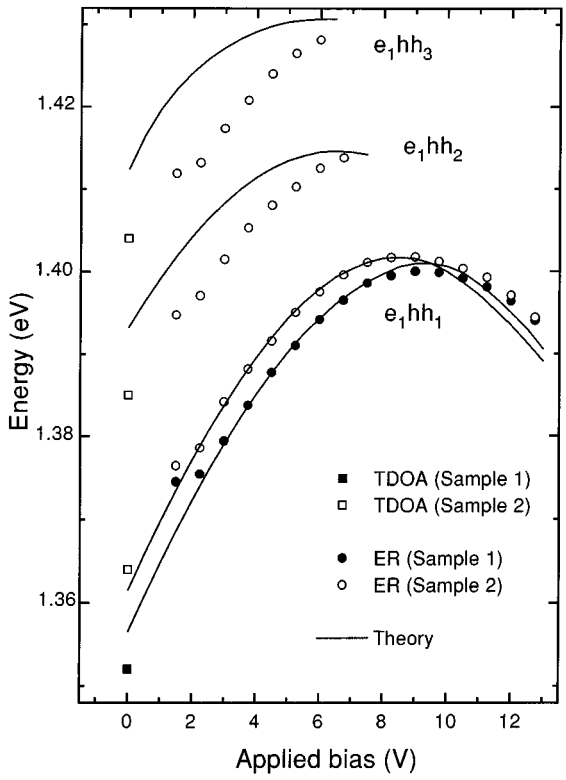

FIG. 4. Experimental excitonic transition energies deduced from TDOA (squares) and from fits to ER spectra (circles) for sample 1 (filled symbols) and sample 2 (hollow symbols). The lines are from theoretical calculations with wells of 95-Å width, indium composition is $x=0.143$ for sample 1 and $x=0.144$ for sample 2; the piezoelectric discontinuity is taken to be 165 kV cm^{-1}. The experimental and theoretical results for e_1hh_2 and e_1hh_3 for sample 1 are not plotted for clarity; they exhibit the same behaviors as those of sample 2.

lombic interaction between the two carriers. This induces a 2D character for the exciton and explains the continuous decrease of α. The e_1hh_2 exciton exhibits the same behaviors as these corresponding to e_1hh_1, but due to the larger extension of the wave function of the second level of hole, the overlap remains and begins to decrease for larger quantum well thicknesses than for e_1hh_1.

V. RESULTS AND DISCUSSION

The experimental transition energies of the fundamental exciton in samples 1 and 2 and the second and third excited excitons in sample 2, obtained from both TDOA and ER are plotted as a function of applied bias in Fig. 4. There is a good agreement between the results from the two spectroscopic techniques; the slight difference between the TDOA data and extrapolations of the energy values deduced from ER for zero bias are attributed to inhomogeneities in the quantum-well thicknesses. (The pieces of the samples used for TDOA are different from these processed for ER.) It can be seen that there is an inversion of the curvature of the ER energy for small voltages ($\approx$2 V). This is due to screening effects; at low bias voltages, the in-well field is stronger and therefore the in-well screening efficiency is a maximum, becoming sufficiently large to increase the excitonic energies by reducing the QCSE.

The best fit to the experimental data is plotted in Fig. 4 and concentrates on the fundamental exciton because it is possible to locate the bias and energy positions of the flat band in the latter case and because the curvature of the experimental points for the e_1hh_2 and e_1hh_3 excitonic energies cannot be well reproduced with any set of fitting parameters. The energy differences between e_1hh_2-e_1hh_1 and e_1hh_3-e_1hh_1 transitions are too large. In addition, the maxima of the theoretical curves occur at lower voltages for e_1hh_2 and e_1hh_3 than for e_1hh_1. These two behaviors suggest that indium surface segregation may occur; its effects are to increase the well width narrowing the sublevels, and to blueshift the excitonic energies enabling the in-well electric field to be increased in our model to push the theoretical curves of the excited excitons to larger bias voltages. This point is now under investigation.

Nevertheless, good agreement is found for the fundamen-

tal exciton in both samples. The parameters used to fit the experimental data are close to the nominal values given by the growth sequences. In agreement with the fits to ER spectra, the width of the wells L_w is estimated to be 95 Å for the two samples. The indium composition x is then found to be 0.143 for sample 1 and 0.144 for sample 2. These two variables, x and L_w, are evaluated simultaneously by considering the energies of the flat band configuration, which can be located unambiguously from the top of the experimental curves plotted in Fig. 4. Thus we assume that the barrier field does not influence the exciton energy,[7] therefore the pair (x,L_w) is determined by calculations for a perfect square well. The third adjustable parameter is the piezoelectric field in the $In_xGa_{1-x}As$ layers; this electric field arises from the product of a piezoelectric constant and a term including the displacements of atoms under a field of deformations induced by the lattice mismatch. Note that if one assumes that the piezoelectric constant of the alloy can be calculated by a simple linear interpolation, the piezoelectric field is therefore determined from the knowledge of the indium composition and is not to be taken as an adjustable parameter. In fact, the piezoelectric field calculated by this formalism is 220 kV cm^{-1} for $x=0.144$, which is inconsistent with our experimental results. This value must be drastically reduced to 165 kV cm^{-1} for a correct description of the experimental excitonic transition energies to be made. The uncertainty in the determination of the piezoelectric field from the latter is 5% and is mainly due to the lack of precision in the estimation of the exact bias for reaching the flat band configuration. Such a discrepancy between theoretical and experimental values of the piezoelectric discontinuity has been already reported in the literature but its origin is still unclear.[15,31–33] Several authors attribute this disagreement to an approximate knowledge of the piezoelectric constants of the binary constituents;[32,33] Tober and Bahder suggest that it may arise from charge accumulation at the interfaces screening the in-well electric field.[15] Other physical effects may be mentioned such as indium surface segregation whose effects on band structure are strongly enhanced by the presence of large built-in electric fields. Note that the paper of Shen *et al.* reports an experimental determination of the value of the piezoelectric field in good agreement with the theoretical prediction.[34] However, the uncertainty given corresponds to the discrepancy between our results and the theory.

Since the in-well electric field is responsible for the shifts of the transition energies, it is necessary to reproduce exactly the curvature in experimental data for an accurate determination of its value and thus of that of the piezoelectric field strength. The variation of the excitonic binding energy takes an important place in this curvature. As can be seen from Fig. 5, the variation in the binding energy with applied bias exceeds 2 meV. Therefore, if excitonic contributions are not taken into account via the binding energy variations with applied bias, the piezoelectric field will be underestimated. From a practical point of view, we have plotted the binding energies obtained from the two variational parameter trial function and the two limited cases in Fig. 5. It can be seen that the choice of model does not really influence the fit. Therefore, the use of the simplest 2D model ($\alpha=0$) that brings numerical results instantaneously appears to be appropriated for a fitting procedure. The values of the two variational parameters also plotted as functions of applied bias follow the physical evolution described above. The Bohr radius increases for large in-well fields due to the enhanced spatial separation of electron and hole leading to a drastic decrease of the Coulombic interaction responsible for the fall in the value of the dimensionality parameter. Note that the fall of α on the large bias side begins before reaching the flat band configuration. This can be explained by the large barrier field that attracts the carriers towards the outside of the quantum well making their wave functions nonsymmetric even in a flat well and reducing slightly their Coulombic interaction.

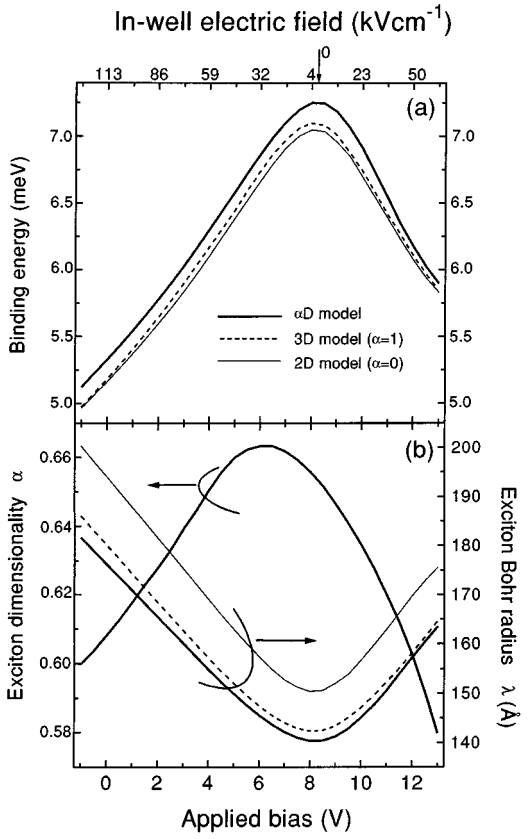

FIG. 5. Excitonic binding energy of the exciton in its fundamental state (a) and the variational parameters α and λ (b), as functions of the applied bias, with $\alpha=0$ (2D model), $\alpha=1$ (3D model), and α variable (αD model).

All the experimental and theoretical results concerning the excitonic oscillator strength values are plotted in Fig. 6 as functions of applied bias for e_1hh_1, e_1hh_2, and e_1hh_3 excitons. The experimental points deduced from the fits to ER spectra are plotted with 15% error bars; most of this relative uncertainty is attributable to that in the damping parameter, which influences drastically the evaluation of the experimental oscillator strength. Theoretical results are also plotted for the two limiting cases $\alpha=0$ and $\alpha=1$ and for the case where α is taken as a variational parameter. The curves obtained in the latter case stand between the others, very close to that obtained by using the 3D exciton model ($\alpha=1$). Such a discrepancy between experimental and theoretical oscillator strengths, which is of the order of a factor of 2, has already been reported in [001]-grown $In_xGa_{1-x}As/GaAs$ quantum wells.[27] However, André *et al.* found good agreement be-

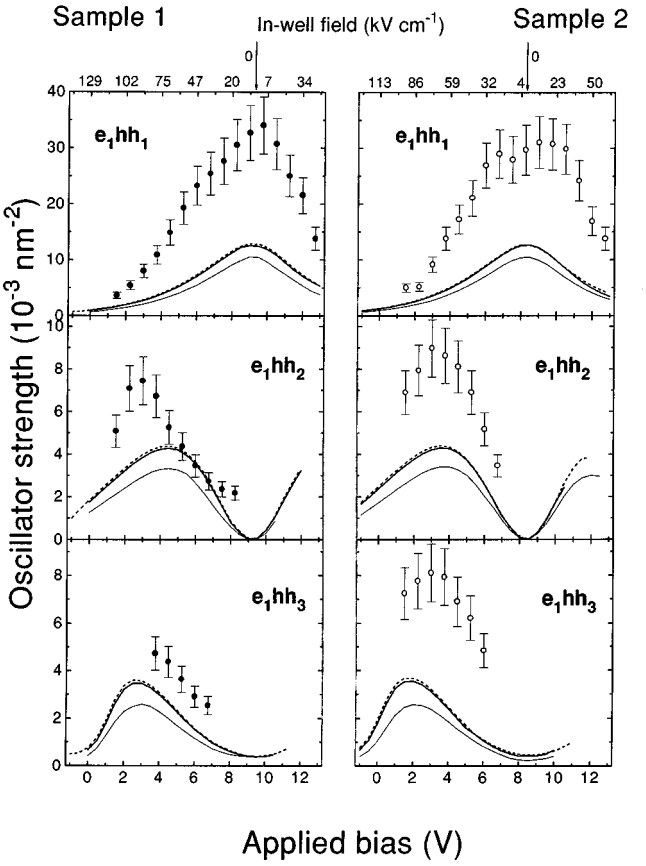

FIG. 6. Oscillator strength as a function of applied bias for the $e_1\mathrm{hh}_1$, $e_1\mathrm{hh}_2$, and $e_1\mathrm{hh}_3$ excitonic transitions in samples 1 and 2. Circles with error bars are experimental data from ER experiments, lines are from variational calculations using $\alpha=1$ (dashed lines), $\alpha=0$ (thin solid lines), and α as a variational parameter (thick solid lines).

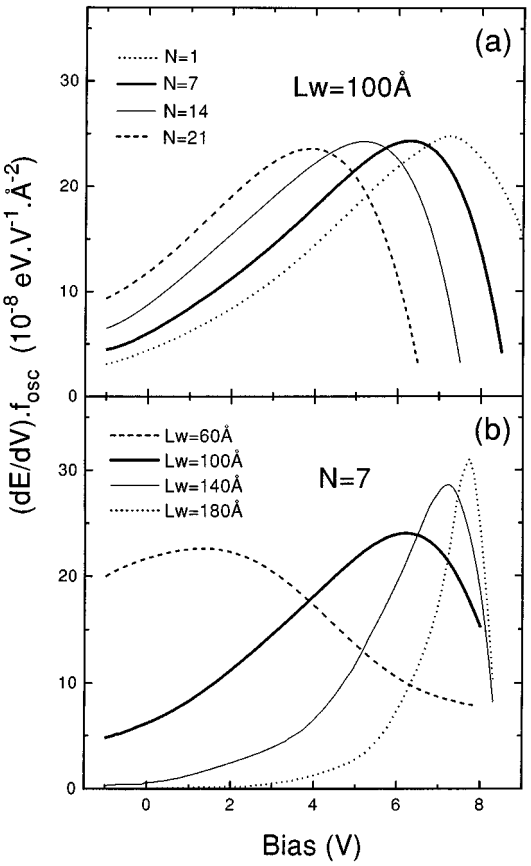

FIG. 7. Plot of the quantity $f_{\mathrm{osc}}dE/dV$, for the fundamental transition, as a figure of merit for optoelectronic devices for 100-Å-thick quantum wells with varying number of wells (a), and for a 7-well heterostructure with different quantum-well thicknesses (b). The piezoelectric field is taken to be 165 kV cm^{-1}.

tween experimental data and calculations, employing the same variational method, in the case of CdTe/Cd_xMn_{1-x}Te quantum wells.[6] The only difference lies in the determination of the hole in-plane effective masses; the valence-band mixing was not taken into account in our calculations. The approximation that consists of the determination of the in-plane hole masses by a simple reduction of the Luttinger Hamiltonian of the bulk $In_xGa_{1-x}As$ to the in-plane components of the wave vector does not appear to be relevant for a quantitative description of the oscillator strength of excitons in strained quantum wells.

However, our model reproduces accurately the physical trends for the variations of the oscillator strengths with applied bias and therefore with in-well field. The maximum for each exciton is well defined and is localized at zero in-well electric field for the fundamental exciton and at a larger field for $e_1\mathrm{hh}_3$ than for $e_1\mathrm{hh}_2$. The fact that the oscillator strengths for all excitons are weak in the high electric field regime confirms the experimental observation that all the excitonic transitions become undetectable for bias less than 1.5 V, corresponding to in-well electric fields exceeding 100 kV cm^{-1}.

This result is of fundamental interest for the design of optoelectronic devices because it shows that increasing the in-well field for an enhanced QCSE, usable to provide large energy shifts, leads to a strong decrease of oscillator strengths of excitonic transitions for the fundamental exciton but also for excitons involving excited levels. It is evident that the best device combines the largest energy shift with the largest oscillator strength for an optimized working. Therefore, and to follow the idea of Rodriguez-Gijones and Rees who considered a figure of merit for all optical devices combining screening efficiency and transition probability,[7] we define a figure of merit for optoelectronic devices that is the product of the energy shift caused by the addition of 1 V applied bias: dE_{exc}/dV and the oscillator strength f_{osc} of the exciton at the bias considered. Considering that the devices are based on the fundamental transition, Fig. 7 shows the variation of the quantity $f_{\mathrm{osc}}dE_{\mathrm{exc}}/dV$ with applied bias for the $e_1\mathrm{hh}_1$ exciton, for different number of wells with 100-Å widths in the heterostructure and for several quantum-well thicknesses in the case of seven wells. The excitonic trial function used to calculate this figure of merit corresponds to that for a pure 3D exciton ($\alpha=1$), the differences between the cases $\alpha=1$ and α variable for exciton binding energies and oscillator strength being very small, and the model with $\alpha=1$ reduces drastically the computing time.

From Fig. 7 it is seen that the quantity $f_{\mathrm{osc}}dE/dV$ passes through a maximum at a given bias and therefore the number of wells and the well width can be adjusted to obtain an optimized working at the command bias. The modification of the number of wells influences only the peak position but

does not act on its shape. Furthermore, the well width plays a role on the bias value, the damping, and the maxima of the curve. A device with narrow wells will work within a larger number of bias values but its efficiency is weaker than a wide-well-based device, which provides a very localized figure of merit and therefore enables a better working in a smaller window of usable bias. In addition, wide well devices work at voltages near the flat band conditions and thus the working of these devices would not be perturbed by excited excitonic transitions. Note that the number of wells plays a role because contributions from all wells add up and thus can be used to balance a weak oscillator strength value. This effect is not taken into account in our analysis as the results are only valid for one of the wells.

VI. CONCLUSION

In this paper we have investigated experimentally and theoretically, within a variational approach, the excitonic properties of piezoelectric multiple-quantum-well *p-i-n* heterostructures grown along the [111] direction. The piezoelectric field in the strained layers is determined by including excitonic contributions. Its value ($165\ \mathrm{kV\ cm^{-1}}$), which is 30% lower than the theoretical prediction, is in good agreement with all the studies reported in the literature. We have shown that the quantum-well thickness influences drastically the excitonic properties of piezoelectric quantum wells. In narrow quantum wells, the perturbation caused by the electric field is weak because of the extension of the carrier wave functions. However, when the well thickness increases, the 2D excitonic character is magnified for both the fundamental and first excited excitons. Simultaneously their binding energies and oscillator strengths fall rapidly because of the quasi-type-II configuration due to enhanced electron and hole spatial separation. We have also shown experimentally and theoretically how the in-well electric field affects the oscillator strengths of excitons in adding bias voltages. This study confirms the allowed or forbidden characters of the excitonic transitions involving fundamental and excited hole levels and demonstrates that, for sufficiently large electric fields, the oscillator strengths for transitions forbidden from classical selection rules become stronger than that for the fundamental transition. In the very high electric field regime, the oscillator strengths for all the excitonic transitions become very weak. We have used a figure of merit for optoelectronic devices combining oscillator strengths and energy shifts in order to optimize the device performances. It is clear that the key parameter is the well width; wide-well-based devices provide better working but reduce the usable range of bias.

*FAX: 33 4 73 40 73 40.
Electronic address: pballet@lasmea.univ-bpclermont.fr

[1] D. L. Smith, Solid State Commun. **57**, 919 (1986).
[2] T. Anan, K. Nishi, and S. Sugou, Appl. Phys. Lett. **60**, 3159 (1992).
[3] K. W. Goossen, E. A. Caridi, T. Y. Chang, J. B. Stark, D. A. B. Miller, and R. A. Morgan, Appl. Phys. Lett. **56**, 715 (1990).
[4] I. W. Tao and W. I. Wang, Electron. Lett. **28**, 705 (1992).
[5] A. S. Pabla, J. L. Sanchez-Rojas, J. Woodhead, R. Grey, J. P. R. David, G. J. Rees, G. Hill, M. A. Pate, P. N. Robson, R. A. Hoog, T. A. Fisher, A. R. K. Willckox, D. M. Whittaker, M. S. Skolnick, and D. J. Mowbray, Appl. Phys. Lett. **63**, 752 (1993).
[6] R. André, J. Cibert, and Le Si Dang, Phys. Rev. B **52**, 12 013 (1995).
[7] P. J. Rodriguez-Girones and G. J. Rees, IEEE Photonics Technol. Lett. **7**, 71 (1995).
[8] R. Grey, J. P. R. David, G. Hill, A. S. Pabla, M. A. Pate, G. J. Rees, P. N. Robson, P. J. Rodriguez-Girones, T. E. Sale, J. Woodhead, T. A. Fisher, R. A. Hogg, D. J. Mowbray, M. S. Skolnick, D. M. Whittaker, and A. R. K. Willckox, Microelectron. J. **26**, 811 (1995).
[9] J. P. R. David, R. Grey, G. J. Rees, A. S. Pabla, T. E. Sale, J. Woodhead, J. L. Sanchez-Rojas, M. A. Pate, G. Hill, P. N. Robson, R. A. Hogg, T. A. Fisher, M. S. Skolnick, D. M. Whittaker, A. R. K. Willckox, and D. J. Mowbray, J. Electron. Mater. **23**, 975 (1994).
[10] A. S. Pabla, J. L. Sanchez-Rojas, J. Woodhead, R. Grey, J. P. R. David, G. J. Rees, G. Hill, M. A. Pate, P. N. Robson, R. A. Hogg, T. A. Fisher, A. R. K. Willckox, D. M. Whittaker, M. S. Skolnick, and D. J. Mowbray, Appl. Phys. Lett. **63**, 752 (1993).
[11] A-M. Vasson, A. Vasson, J. Leymarie, P. Disseix, P. Boring, and B. Gil, Semicond. Sci. Technol. **8**, 303 (1993).
[12] D. Boffety, J. Leymarie, A. Vasson, A-M. Vasson, C. A. Bates, J. M. Chamberlain, J. L. Dunn, M. Henini, and O. H. Hughes, Semicond. Sci. Technol. **8**, 1408 (1993).
[13] B. V. Shanabrook, O. J. Glembocki, and W. T. Beard, Phys. Rev. B **35**, 2540 (1987).
[14] L. C. Andreani and A. Pasquarello, Phys. Rev. B **42**, 8928 (1990).
[15] R. L. Tober and T. B. Bahder, Appl. Phys. Lett. **63**, 2369 (1993).
[16] E. A. Caridi, T. Y. Chang, K. W. Goosen, and L. F. Eastman, Appl. Phys. Lett. **56**, 659 (1990).
[17] K. Yang, T. Anan, and L. J. Schowalter, Appl. Phys. Lett. **65**, 2789 (1994).
[18] *Semiconductors Physics of Group IV Elements and III-V Compounds*, O. Madelung, Landolt-Börnstein, New Series, Group III, Vol. 17, Pt. a (Springer, New York, 1982).
[19] A. R. Goni, K. Strössner, K. Syassen, and M. Cardona, Phys. Rev. B **36**, 1581 (1987).
[20] R. People and K. Sputz, Phys. Rev. B **41**, 8431 (1990).
[21] J. M. Luttinger, Phys. Rev. **102**, 1030 (1956).
[22] J. Los, A. Fasolino, and A. Catellani, Phys. Rev. B **53**, 4630 (1996).
[23] R. Winkler and A. I. Nesvizhskii, Phys. Rev. B **53**, 9984 (1996).
[24] T. S. Moise, L. J. Guido, and R. C. Barker, Phys. Rev. B **47**, 6758 (1993).
[25] K. H. Goetz, D. Bimberg, H. Jürgensen, J. Selders, A. V. Solomonov, G. F. Glinskii, and M. Razeghi, J. Appl. Phys. **54**, 4543 (1983).
[26] W. W. Lui and M. Fukuma, J. Appl. Phys. **60**, 1555 (1986).
[27] C. Monier, P. Disseix, J. Leymarie, A. Vasson, A-M. Vasson, B. Courboules, C. Deparis, M. Leroux, and J. Massies, *Semiconductor Heteroepitaxy*, edited by B. Gil and R. L. Aulombard (World Scientific, Singapore, 1995), p. 511.
[28] P. Disseix, J. Leymarie, A. Vasson, A-M. Vasson, C. Monier, N. Grandjean, M. Leroux, and J. Massies, Phys. Rev. B **55**, 2406 (1997).
[29] P. Bigenwald, B. Gil, and P. Boring, Phys. Rev. B **48**, 9122 (1993).

[30] P. Ballet, P. Disseix, A. Vasson, A-M. Vasson, and R. Grey, Microelectron. J. (to be published) (special issue on novel index semiconductor surfaces).
[31] R. A. Hogg, T. A. Fisher, A. R. K. Willcox, D. M. Whittaker, M. S. Skolnick, D. J. Mowbray, J. P. R. David, A. S. Pabla, G. J. Rees, R. Grey, J. Woodhead, J. L. Sanchez-Rojas, G. Hill, M. A. Pate, and P. N. Robson, Phys. Rev. B **48**, 8491 (1993).
[32] J. L. Sanchez-Rojas, A. Sacedon, F. Gonzalez-Sanz, E. Calleja, and E. Munoz, Appl. Phys. Lett. **65**, 2042 (1994).
[33] P. D. Berger, C. Bru, Y. Baltagi, T. Benyattou, M. Berenguer, G. Guillot, X. Marcadet, and J. Nagle, Microelectron. J. **26**, 827 (1995).
[34] H. Shen, M. Dutta, W. Chang, R. Moerkirk, D. M. Kim, K. W. Chung, P. P. Ruden, M. I. Nathan, and M. A. Stroscio, Appl. Phys. Lett. **60**, 2400 (1992).